A TWO-THRESHOLDS EM-MRF ALGORITHM FOR CHANGE DETECTION OF MULTI-TEMPORAL ERS-2 SAR IMAGES

Ya-Qiu Jin
Key Laboratory of Wave Scattering and Remote Sensing Information (Ministry of Education)
Fudan University, Shanghai 200433, China
Email: yqjin@fudan.ac.cn

KEY WORDS: Multi-temporal SAR, Two thresholds EM, MRF, Change detection

ABSTRACT:

To automatically detect and analyze the surface change in the urban area from multi-temporal SAR images, an algorithm of two-thresholds EM (Expectation Maximum) and MRF (Markov Random Field) is developed. Difference of the SAR images demonstrates variation of backscattering caused by the surface change over all image pixels. Two thresholds are obtained by the EM iterative process and are applied to three classes: enhanced scattering, reduced scattering and no changed regimes. Initializing from the EM result, the ICM (Iterated Conditional Modes) algorithm of the MRF is then applied to analysis of the contexture change detection in the urban area. As an example, two images of the ERS-2 SAR in 1996 and 2002 years over the Shanghai City are studied.

1. INTRODUCTION

The development of the urban areas is a great topic for human civilization in this century. Changes of the urban area such the buildings, roads, greenbelts, botanic zoology, water body, population migration, and local climate etc. need to be accurately assessed. Multi-temporal observations of space-borne remote sensing imagery provide the fast and practical technical means to survey and assess such vast changes. One of the direct applications is to detect and classify the change information of the terrain surfaces [1-5]. The advancement of the SAR (Synthetic Aperture Radar) imagery technology during the latest twenty years, such as SIR-C SAR, ERS-1, 2, RADARSAT, has provided the high-resolution and all weather image data over many years. It becomes feasible to retrieve some information of the terrain surfaces change from space-borne observation.

It is difficult to make manual and intuitive assessment for huge amount of multi-temporal image data over a vast area. Such assessment based on qualitative gray-level analysis cannot be accurate and might lose some important information. It has been a key issue in remote sensing how to automatically detect and analyze the change information of the terrain surfaces. There are usually two methods: the supervised and unsupervised approaches. The former needs a mass of multi-temporal ground truth data for the training samples of classification procedure. The latter performs the change detection by making a direct comparison of the multi-temporal remote sensing images without relying on any additional information. Our paper adopts the unsupervised approach. Rignot and van Zyl [1] made a work of change detection from the difference of two SAR images. Singh [2] performed the statistical analysis of the change vector of infrared multi-channel data for surface change detection. In fact, empirical or manual trial-and-error procedures to make the thresholds for the image difference might loss the reliability and accuracy.

Based on the Bayes theory and Markov model, Bruzzone and Prieto [3] proposed the Expectation Maximum (EM) algorithm and Markov Random Field (MRF) analysis. Two classes: changed and no-changed regimes are classified.

However, their approach has not been validated by using real SAR observations. Moreover, so-called changed might have different meaning. For example, the backscattering was reduced when the area of roughly distributed buildings became as flat grassland, or vice versa, the backscattering was increased when the flat surface turns to a group of buildings or many trees. One ±db change in backscattering might contain different content.

In this paper, two-thresholds EM and MRF algorithm is developed to detect the change of backscattering enhanced, no-changed and reduced regimes from the SAR difference image. Two ERS-2 SAR images in 1996 and 2002 over Shanghai city are analyzed. The results well illustrate the change of the Shanghai area during the years. It might be proposed that multi-thresholds EM and MRF analysis is tractable when multi-polarization, multi-channels, multi-sensors multi-temporal image data become available.

2. THE EM ALGORITHM

Consider two co-registered images X_1 and X_2 with size $I \times J$ at two different times (t_1, t_2). Their difference image is $X = (X_2 - X_1)$. Let X be a random variable to represent the value of $I \times J$ pixels in $X_D = \{X(i, j),\ 1 \le i \le I, 1 \le j \le J\}$.

The change detection and analysis for the difference image is usually to distinguish two opposite classes: unchanged class ω_n and changed class ω_c. The probability density function $p(X)$ of the pixel value in the difference image X_D was modeled as a mixture distribution of two density components associated with ω_n and ω_c, i.e.

$$p(X) = p(X \mid \omega_n)P(\omega_n) + p(X \mid \omega_c)P(\omega_c) \qquad (1)$$

where $P(\omega_n)$, $P(\omega_c)$ of the classes ω_n and ω_c are the *a priori* probabilities. $p(X \mid \omega_k)(k = n, c)$ is the conditional probability density functions. The unsupervised estimations of $p(X \mid \omega_n)$, $p(X \mid \omega_c)$, $P(\omega_n)$ and $P(\omega_c)$ can be performed by the expectation maximum (EM) algorithm. The EM algorithm is a general approach to maximum likelihood (ML) estimation for incomplete data problems [6-8]. It consists of an expectation step and a maximization step. The expectation step is computed with respect to the unknown underlying variable using the estimates of the parameters conditioned by observations. The maximization step provides new estimates of the parameters.

The EM algorithm follows Bruzzone and Prieto [3].

3. TWO-THRESHOLDS EM

The pixels value of SAR image represents the echo power (backscattering σ^0) of the radar observation. The difference image (i.e. $X = \sigma_D^0 = \sigma_2^0 - \sigma_1^0$) can show where the backscattering is enhanced ($\sigma_D^0 > 0$), unchanged ($\sigma_D^0 \approx 0$) or reduced ($\sigma_D^0 < 0$). This classification is applicable to information retrieval of the terrain surfaces change. We classify the pixels of the difference image into three classes: σ_D^0-enhanced ω_{c1}, σ_D^0-unchanged ω_n

and σ_D^0 -reduced ω_{c2}, i.e. three subsets of pixels with $\sigma_D^0 > 0$, around 0 and $\sigma_D^0 < 0$.

Thus, the probability density function $p(X)$ of X_D is modeled as a mixture density distribution consisting of three components:

$$\begin{aligned} p(X) &= p(X \mid \omega_{c1})P(\omega_{c1}) \\ &+ p(X \mid \omega_n)P(\omega_n) + p(X \mid \omega_{c2})P(\omega_{c2}) \end{aligned} \quad (2)$$

We first obtain T_{o1} by applying the EM algorithm to the enhanced class ω_{c1} and no-enhanced class ω_{n1} (ω_n and ω_{c2}). Then, we obtain T_{o2} by applying the EM to the reduced class ω_{c2} and no-reduced class ω_{n2} (ω_n and ω_{c1}), where $\omega_{n1} = \omega_n \cup \omega_{c2}$, $\omega_{n2} = \omega_n \cup \omega_{c1}$. Finally, the two results are superposed to get the final classification.

Figure 1 shows the grayscale histogram of the difference image from the ERS-2 SAR image data (which is the difference of Figures 2 and 3) around the Yan Zhong greenbelt of Shanghai downtown center. Three classes of the probability distributions are outlined in this figure. The histogram is normalized in accordance with the probability density distributions. The subset S_{n1} likely belong to the class ω_{n1} and the subset S_{c1} likely belong to class ω_{c1} are obtained by applying two-thresholds T_{n1} and T_{c1} in the enhanced regime ($X \geq 0$) of the histogram $h(X)$. T_{n1} and T_{c1} are expressed as $T_{n1} = M_{D1}(1-\gamma)$ and $T_{n1} = M_{D1}(1+\gamma)$, where M_{D1} is the mean value of the enhanced regime in $h(X)$ (i.e. $M_{D1} = [\max\{X_D\}/2]$).

Analogously, the subset S_{n2} likely belong to the class ω_{n2} and the subset S_{c2} likely belong to the class ω_{c2} are obtained in the reduced regime ($X < 0$) in the $h(X)$, where $M_{D1} = [\min\{X_D\}/2]$. In this paper, γ = 0.5 is chosen.

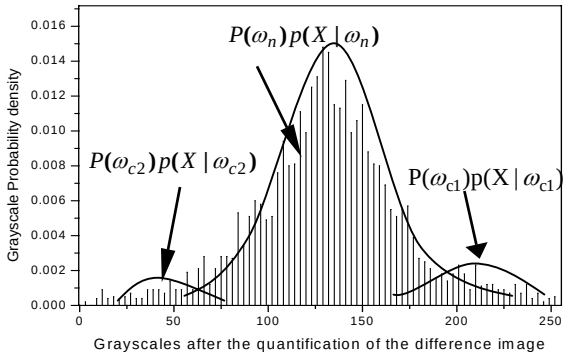

Figure 1. Normalized histogram for 3 classes from difference image data.

We first derive the initial statistical parameters of the subsets $S_{n1} = \{X(i,j) \mid 0 < X(i,j) < T_{n1}\}$, $S_{c1} = \{X(i,j) \mid X(i,j) > T_{c1}\}$, and then derive the parameters of

$S_{n2} = \{X(i,j) \mid T_{n2} < X(i,j) < 0\}$, $S_{c2} = \{X(i,j) \mid X(i,j) < T_{c2}\}$. The initial statistical parameters are related to the classes ω_{n1}, ω_{c1} and the classes ω_{n2}, ω_{c2}, respectively.

Then, EM algorithm of [3] is sequentially used to perform the iterations on the four classes, i.e. the *a priori* probability and statistical parameters [$P(\omega_{n1})$, μ_{n1}, σ_{n1}^2], [$P(\omega_{c1})$, μ_{c1}, σ_{c1}^2], [$P(\omega_{n2})$, μ_{n2}, σ_{n2}^2], [$P(\omega_{c2})$, μ_{c2}, σ_{c2}^2] . The thresholds T_{o1} and T_{o2} are then obtained.

4. THE MRF SPATIAL-CONTEXTUAL CLASSIFICATION

As Bruzzone and Prieto [3] discussed for the MRF approach, the pixels of the image are spatially correlated, i.e. a pixel belonging to the class ω_k is likely to be surrounded by pixels belonging to the same class. To take account of spatial contexture may yield more reliable and accurate change detection.

Let the set $C = \{C_l, 1 \leq l \leq L\}$ to represent the possible sets of the labels in the difference image, where $C_l = \{C_l(i,j), 1 \leq i \leq I, 1 \leq j \leq J\}$, $C_l(i,j) \in \{\omega_{c1}, \omega_{c2}, \omega_n\}$, $L = 3^{IJ}$, I, J is the height and width of difference image respectively.

According to the Bayes rule for minimum error, the classification result should maximize the posterior conditional probability,

$$C_k = \arg\max_{C_l \in C}\{P(C_l \mid X_D)\} = \arg\max_{C_l \in C}\{P(C_l)p(X_D \mid C_l)\} \quad (3)$$

where X_D is the difference image, $P(C_l)$ is the prior model for the class labels, and $p(X_D \mid C_l)$ is the joint density function of the pixel values in the difference image given the set of labels C_ℓ. The solution of Eq. (3) requires the MRF approach to estimate both of $P(C_l)$ and $p(X_D \mid C_l)$.

In order to formulate the problem by using the MRF, it is necessary to introduce the concept of a spatial neighborhood system defining by N. Considering a pixel (i,j), its neighborhood can be expressed:

$$N(i,j) = \{(i,j) + (\nu,\varsigma), (\nu,\varsigma) \in N\} \quad (4)$$

in this paper , $N = \{(\pm 1, 0), (0, \pm 1), (1, \pm 1), (-1, \pm 1)\}$, i.e., the neighborhood of one pixel is composed of the eight pixels surrounding it.

Let $C_\ell(i,j)$ represent the class label of (i,j), $C_{\ell N}$ represent the class labels of the neighborhood pixels of (i,j), and $C_{\ell_{|(i,j)}}$ represent the class labels of the pixels in the difference image except (i,j). If we take C_ℓ as a MRF, C_ℓ has two properties as follows:

$$P(C_\ell) > 0 \ , \quad \forall C_\ell(i,j) \in \{\omega_{c1}, \omega_{c2}, \omega_n\} \quad (5)$$

$$P(C_\ell(i,j) \mid C_{\ell_{|(i,j)}}) = P(C_\ell(i,j) \mid C_{\ell N}) \quad (6)$$

Cliques are referred to the connected sub-graph of neighboring pixels including the center pixel in the neighborhood system. In this paper, only single-pixel and two-pixel cliques are considered. The single-pixel clique has one form, and the two-pixel clique has four forms, the mathematical expressions are respectively, written as

$$L_1 = (i,j) \ , \quad L_2 = \{\{(i,j),(g,h)\} \mid (g,h) \in N_i(i,j)\} .$$

According to the Hammersley-Clifford theorem, MRF is equivalent to Gibbs distribution. Therefore, the conditional probability of the class label of (i,j) given the pixel labels elsewhere is expressed as [3]

$$\begin{aligned} &P(C_\ell(i,j) \mid \{C_\ell(g,h), (g,h) \neq (i,j)\}) \\ &= P(C_\ell(i,j) \mid \{C_\ell(g,h), (g,h) \in N(i,j)\}) \\ &= \frac{1}{Z}\exp[-U(C_\ell(i,j) \mid \{C_\ell(g,h), (g,h) \in N(i,j)\})] \end{aligned} \quad (7)$$

where $U(\cdot)$ is the Gibbs energy function, and Z is the normalizing factor,

$$Z = \sum_{(g,h)\in\{(i,j)\cup N(i,j)\}} \exp[-U(C_\ell(i,j)\,|\,\{C_\ell(g,h)\})] \tag{8}$$

$$U(C_\ell \,|\, X_D) = \sum_{1\le i\le I}\sum_{1\le j\le J} U(C_\ell(i,j)\,|\,C_{\ell|(i,j)}, X_D) = \sum_{1\le i\le I}\sum_{1\le j\le J} U(C_\ell(i,j)\,|\,C_{\ell N}, X_D) \tag{9}$$

In the Guassian case,

$$U(C_\ell(i,j)\,|\,C_{\ell N}, X_D) = \frac{1}{2}\ln|2\pi\sigma^2_{C_\ell(i,j)}| + \frac{(X(i,j)-\mu_{C_\ell(i,j)})^2}{2\sigma^2_{C_\ell(i,j)}} + v_1(C_\ell(i,j)) + \sum_{(g,h)\in N(i,j)} v_2(C_\ell(i,j), C_\ell(g,h)) \tag{10}$$

where

$$v_1(C_\ell(i,j)) = \alpha\,, \quad (i,j)\in L_1 \tag{11}$$

here α is the weight value of single-pixel clique, and we assume $\alpha = 0$.

$$v_2(C_\ell(i,j), C_\ell(g,h)) = \begin{cases} -\beta, & C_\ell(i,j) = C_\ell(g,h), \{(i,j),(g,h)\}\in L_2 \\ \beta, & C_\ell(i,j) \ne C_\ell(g,h), \{(i,j),(g,h)\}\in L_2 \end{cases} \tag{12}$$

where β is the weight value of two-pixel clique, $0.7 < \beta < 1.5$, in our calculation $\beta = 1.0$.

Generation of the final change-detection map involves the labeling of all the pixels in the difference image so that the posterior probability is maximized. In terms of Markov models, this is equivalent to the minimization of the following energy function

$$U(C_\ell \,|\, X_D) = \sum_{1\le i\le I}\sum_{1\le j\le J}[U_I(X(i,j)/C_\ell(i,j)) + U_C(C_\ell(i,j)/\{C_\ell(g,h),(g,h)\in N(i,j)\})] \tag{13}$$

where $U_C(\cdot)$ describes the inter-pixel class dependence, which is given by the last two terms in Eq.(10). $U_I(\cdot)$ represents the energy function under the assumption of conditional independences, as defined by the first two terms in Eq.(10).

$$U_I(X(i,j)/C_\ell(i,j)) = \frac{1}{2}\ln\left|2\pi\sigma^2_{C_\ell(i,j)}\right| + \frac{1}{2}(X(i,j)-\mu_{C_\ell(i,j)})^2[\sigma^2_{C_\ell(i,j)}]^{-1} \tag{14}$$

where $\sigma^2_{C_\ell(i,j)} \in \{\sigma^2_{c1}, \sigma^2_{c2}, \sigma^2_n\}$, $\mu_{C_\ell(i,j)} \in \{\mu_{c1}, \mu_{c2}, \mu_n\}$ have been obtained by the EM algorithm.

Generally, the solution of Eq. (13) requires an iterative algorithm (e.g., the simulated annealing algorithm). In this paper, we employ the ICM algorithm [9], which has been proved computationally economical and fast convergent to a local minimum of the energy function. The mathematical expression of ICM algorithm can be written as

$$C_\ell = ICM(\alpha, \beta, \mu_{C_\ell(i,j)}, \sigma^2_{C_\ell(i,j)}, X_D, C_{\ell 0}) \tag{15}$$

where $C_{\ell 0}$ is the initial value of C_ℓ.

C_ℓ is obtained by the following steps:

(a) Obtain $C_{\ell 0}$ by the EM algorithm, and initialize C_ℓ with $C_{\ell 0}$.

(b) Calculate new $C_\ell(i,j)$ that minimizes the energy function in Eq. (13).

(c) Repeat step (b) until convergence is reached.

The convergence condition of ICM algorithm is either iterative cycles exceed 30 or less than $\sqrt{IJ}/20$ pixels change. The details of ICM algorithm can be referred to Besag [9].

5. EXAMPLE FOR ERS-2 SAR DATA

Figures 2 and 3 present two image data of ERS-2 SAR in June 4, 1996 and April 9, 2002 over Shanghai China, respectively. The image resolution is 12.5m×12.5m. The images have been co-registered, and the noise is simply reduced by applying a mean filtering (3×3 window size).

We apply the EM algorithm to the difference image of Figures 2 and 3 to iteratively obtain the *a prior* probability and other statistical parameters. Iterative process is sequentially applied to the first and second classes and is quickly converged. Two-thresholds T_{o1}, T_{o2} for surface change detection are then computed. In our example, it yields $T_{o1} = 0.946\times10^{-4}$ and $T_{o2} = -1.013\times10^{-4}$ (the maximum $\sigma^0_D|_{\max} = 5.202\times10^{-4}$ and the minimum $\sigma^0_D|_{\min} = -3.381\times10^{-4}$).

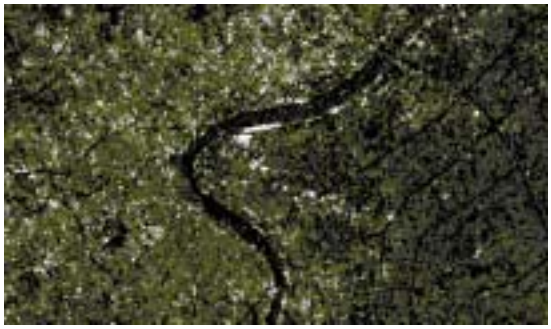

Figure 2. ERS-2 SAR image on June 4, 1996, Shanghai.

Figure 3. ERS-2 SAR image on April 9, 2002, Shanghai.

Figure 4 shows change detection by utilizing the EM algorithm. The white pixels indicate the enhanced area, the black pixels show the reduced places, and the gray area means no-change. This result is significantly different from original difference image.

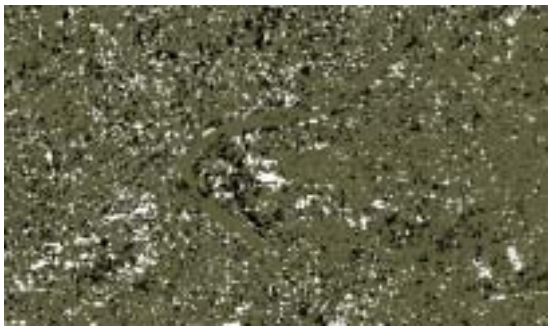

Figure 4. Change detection using two-thresholds EM.

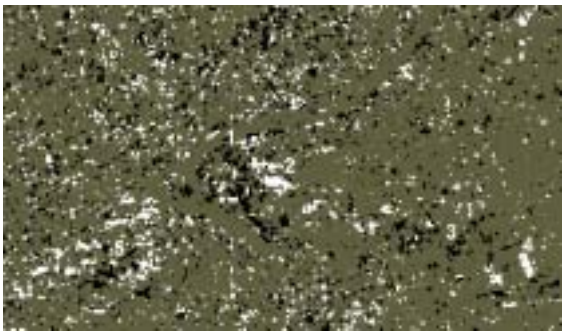

Figure 5. Change detection using ICM algorithm based on MRF.

Figure 5 shows the spatial-contextual change based on the MRF-ICM algorithm. Comparing with Fig.4, it can be seen that the pixels of the same class are more merged and the isolated pixels become much less.

In Figure 5, the black areas marked by the odd number (1,3,5) are the scattering-reduced areas, and the white areas marked by the even number (2,4) are the scattering-enhanced areas. For example, the area 1 is the Lu Jia Zui greenbelt, the area 3 is the Pu Dong Park, and the area 5 is the Yan Zhong greenbelt, where the flat green surface caused less scattering. But, the area 2 is the commercial center at the Lu Jia Zui, where there are many different buildings causing more electromagnetic wave double-reflection and enhance scattering. The area 4 is the location of the new buildings of International Exhibition Center of Shanghai. The areas 1-5 are newly rebuilt after 1996 and are well shown in the change detection of 2002-1996 years data.

It is interesting to overlap Figure 5 over the Shanghai tourist map and identify detailed changes along the city streets during these years from Figure 6.

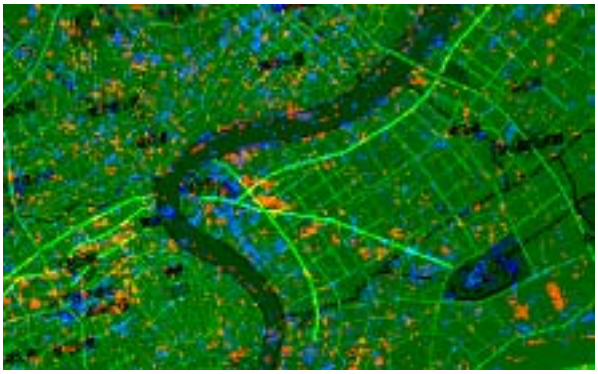

Figure 6. Change overlap to the Shanghai tourist map.

ACKNOWLEDGMENTS

This work was supported by he China State Major Basic Research Project 2001CB309401, 05, and CNSF 60171009，and the Shanghai Optical Sci./Tech. Project 036105012.

REFERENCES

[1] Rignot, E., van Zyl, J. (1993), Change detection techniques for ERS-1 SAR data, *IEEE Trans. Geosci. Remote Sens.*, 31 (4), 896-906.

[2] Singh, A. (1989), Digital change detection techniques using remotely-sensed data, *Int. J. Remote Sens.*, 10 (6), 989-1003.

[3] Bruzzone, L., Prieto, D.F. (2000), Automatic analysis of the difference image for unsupervised change detection, *IEEE Trans. Geosci. Remote Sens.*, 38(3), 1171-1182.

[4] Merril, K.R., Jiajun, L. (1998), A comparison of four algorithms for change detection in an urban environment, *Remote Sens. Environ.*, 63, 95-100.

[5] Kasetkasem, T., and Varshney, P. (2002), An image change detection algorithm based on Markov random field model", 2002, *IEEE Trans. Geosci. Remote Sens.*, 40 (8): 1815-1823.

[6] Dempster, A.P., Laird, N.M., Rubin, D.B. (1977), Maximum linkelihood from incomplete data via the EM algorithm, *J. Roy. Statist. Soc.*, 39 (1), 1-38.

[7] Moon, T.K. (1996), The expectation-maximization algorithm, *Signal Processing Mag.*, 13 (6), 47-60.

[8] Render, A.P., Walker, H.F. (1984), Mixture densities, maximum likelihood and the EM algorithm, *SIAM Review*, 26(2), 195-239.

[9] Besag, J. (1986), On the statistic analysis of dirty pictures, *J. Royal Statist. Soc., series B*, 48, 259-302.